

advances.sciencemag.org/cgi/content/full/6/15/eaax5150/DC1

Supplementary Materials for

Histone deacetylases 1 and 2 silence cryptic transcription to promote mitochondrial function during cardiogenesis

Zachary J. Milstone, Sherin Saheera, Lauren M. Bourke, Tomer Shpilka, Cole M. Haynes, Chinmay M. Trivedi*

*Corresponding author. Email: chinmay.trivedi@umassmed.edu.

Published 10 April 2020, *Sci. Adv.* **6**, eaax5150 (2020)
DOI: 10.1126/sciadv.aax5150

This PDF file includes:

Supplementary Materials and Methods
Supplementary Text
Figs. S1 to S5

Supplementary Materials

Materials and Methods

Mitochondrial DNA (mtDNA)/Nuclear DNA (nDNA) Quantification

Primers for mtDNA/nDNA Quantification		
Target	Forward (5' – 3')	Reverse (5' – 3')
mMito	CTAGAAACCCCGAAACCAA	CCAGCTATCACCAAGCTCGT
nDNA	ATGGGAAGCCGAACATACTG	CAGTCTCAGTGGGGGTGAAT

Primers taken from: Malik, Afshan N., Anna Czajka, and Phil Cunningham. 2016. “Accurate Quantification of Mouse Mitochondrial DNA without Co-Amplification of Nuclear Mitochondrial Insertion Sequences.” *Mitochondrion* 29 (July): 59–64.

Rapid Amplification of cDNA Ends (RACE)

Primers for 5'RACE	
Target	Reverse ((5' – 3'))
CS (Exon 5)	GGCTGCAACGCACGGCAGCTTGGCA
Ndufb9 (Exon 4)	TGGGCCGTTCCCGAGGTCTGGTCACA

Chromatin Immunoprecipitation Quantitative PCR (ChIP-qPCR)

Primers for ChIP-qPCR Analysis		
Target	Forward (5' – 3')	Reverse (5' – 3')
CS TSS ^C	CCATTTTGGGCCAATGGTCTG	GGGGAAGGGTAGACAAACCG
CS TSS ^A	AAGTGCCACACTGTAAGCCT	GGACAGCCTGAGTGAGTTTGA
Ndufb9 TSS ^C	GAGGCTCACGACCAAGACAA	GGAACCGGAAGGACGAGC
Ndufb9 TSS ^{A1}	TGCACCGTGCTGTTACTGAT	ACCTCATCAACTTCAGGCCG
Ndufb9 TSS ^{A2}	AGCAGCCCCTTGAGTTTTGT	GCTTCTCAGAGGGATGCCA

Quantitative Reverse Transcription PCR (RT-qPCR)

Primers for Early/Late Exon Quantification		
Target	Forward (5' – 3')	Reverse (5' – 3')
Gapdh	ATGTTCCAGTATGACTCCACTCACG	GAAGACACCAGTAGACTCCACGACA
CS Early	TTGGGAGCCAAGAACTCATCCTG	TCATGTCCACAGTGATCTGGC
CS Late 6-7	ACAGTGAAAGCAACTTCGCC	TCAATGGCTCCGATACTGCTG
Ndufb9 Early	GAAGGTGCTGCGGCTGTATAA	TACCGGTACTGTCCCTGTGG
Ndufb9 Late	GGCATCCCTCTGAGAAAGCA	GCTTAACCTCCCGATCCCAG

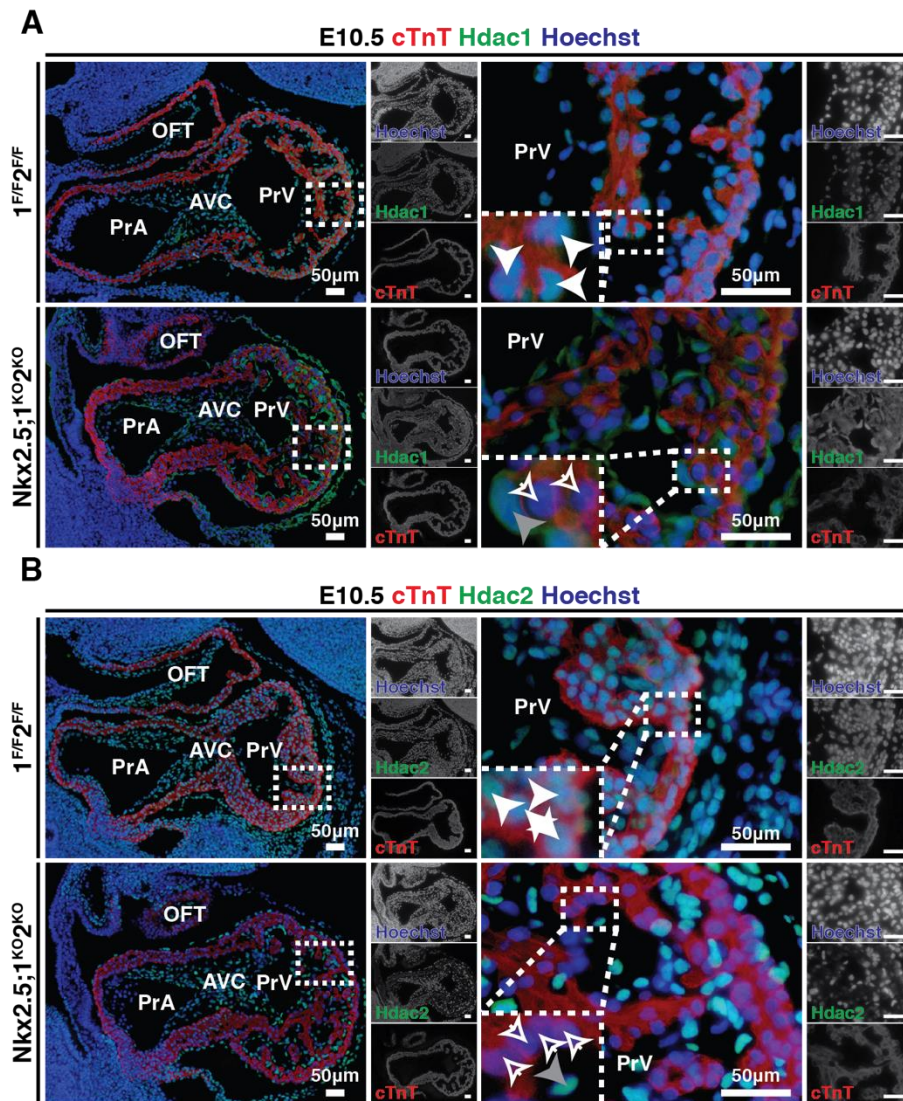
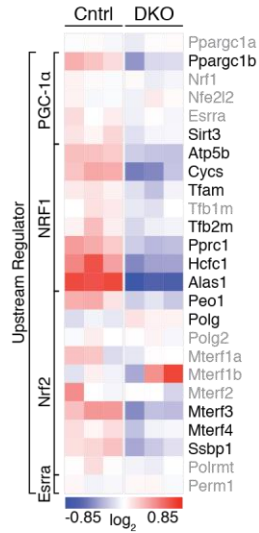


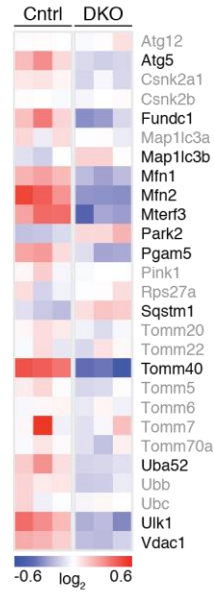
Fig. S1. Complete loss of Hdac1 and Hdac2 in primitive heart tube cardiomyocytes by E10.5.

(A-B) Hdac1 (A) and Hdac2 (B) staining on *Nkx2.5;1^{KO}/2^{KO}* and *1^{FF}/2^{FF}* E10.5 sagittal sections at AVC level with cardiac troponin (cTnT) and Hoechst nuclear counterstain (solid white arrows, Hdac1⁺ or Hdac2⁺ cardiomyocytes; hollow white arrows, Hdac1⁻ or Hdac2⁻ cardiomyocytes; gray arrows, Hdac1⁺/cTnT⁻ or Hdac2⁺/cTnT⁻ cells). Grayscale images are unedited. OFT, outflow tract; PrA, primitive atria; AVC, atrioventricular canal; PrV, primitive ventricle.

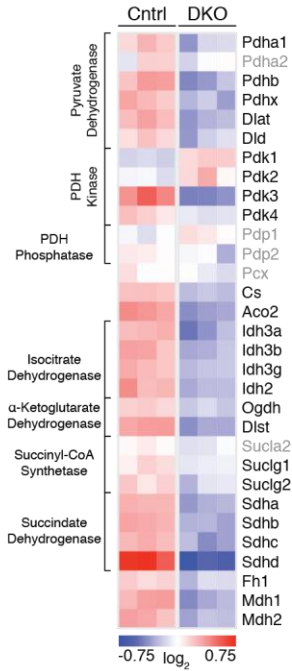
A Mitochondrial Biogenesis (R-MMU-1592230)



B Mitophagy (R-MMU-5205647)



C TCA Cycle (WP434)



D

Electron Transport Chain (WP295)

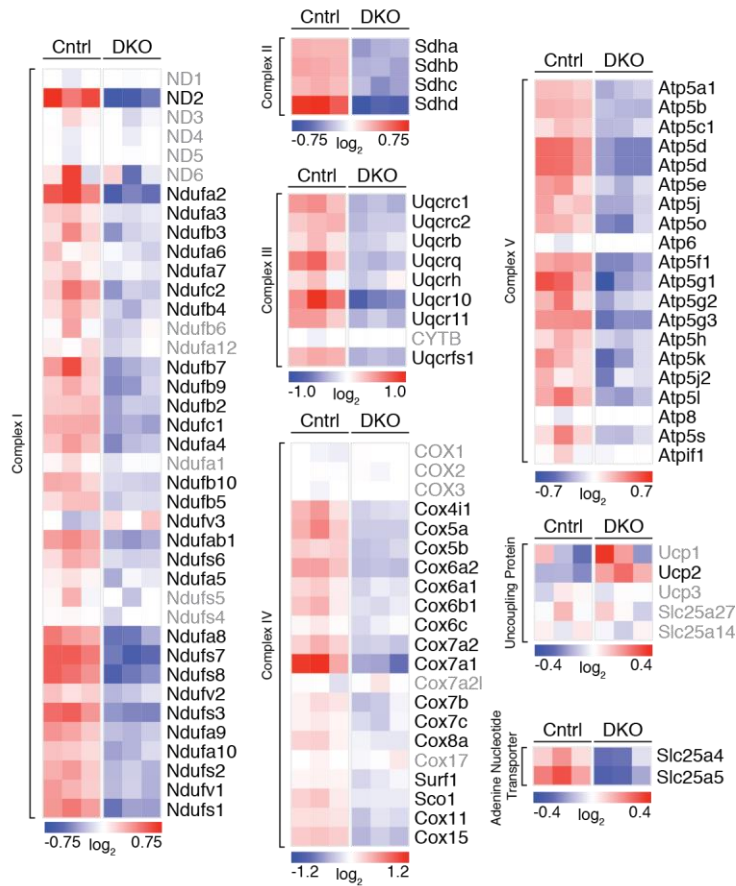


Fig. S2. Loss of Hdac1/Hdac2 causes downregulation of metabolic and cardiac gene programs without concordant upstream changes.

(A) Heatmap of Mitochondrial Biogenesis Reactome gene set (R-MMU-1592230). (B) Heatmap of Mitophagy Reactome gene set (R-MMU-5205647). (C) Heatmap of Tricarboxylic Acid Cycle (TCA Cycle) WikiPathways gene set (WP434). (D) Heatmap of Electron Transport Chain WikiPathways gene set (WP295) separated by individual chain components/complexes. Black text, significantly changed (FDR<0.05); gray text, not significantly changed (FDR>0.05).

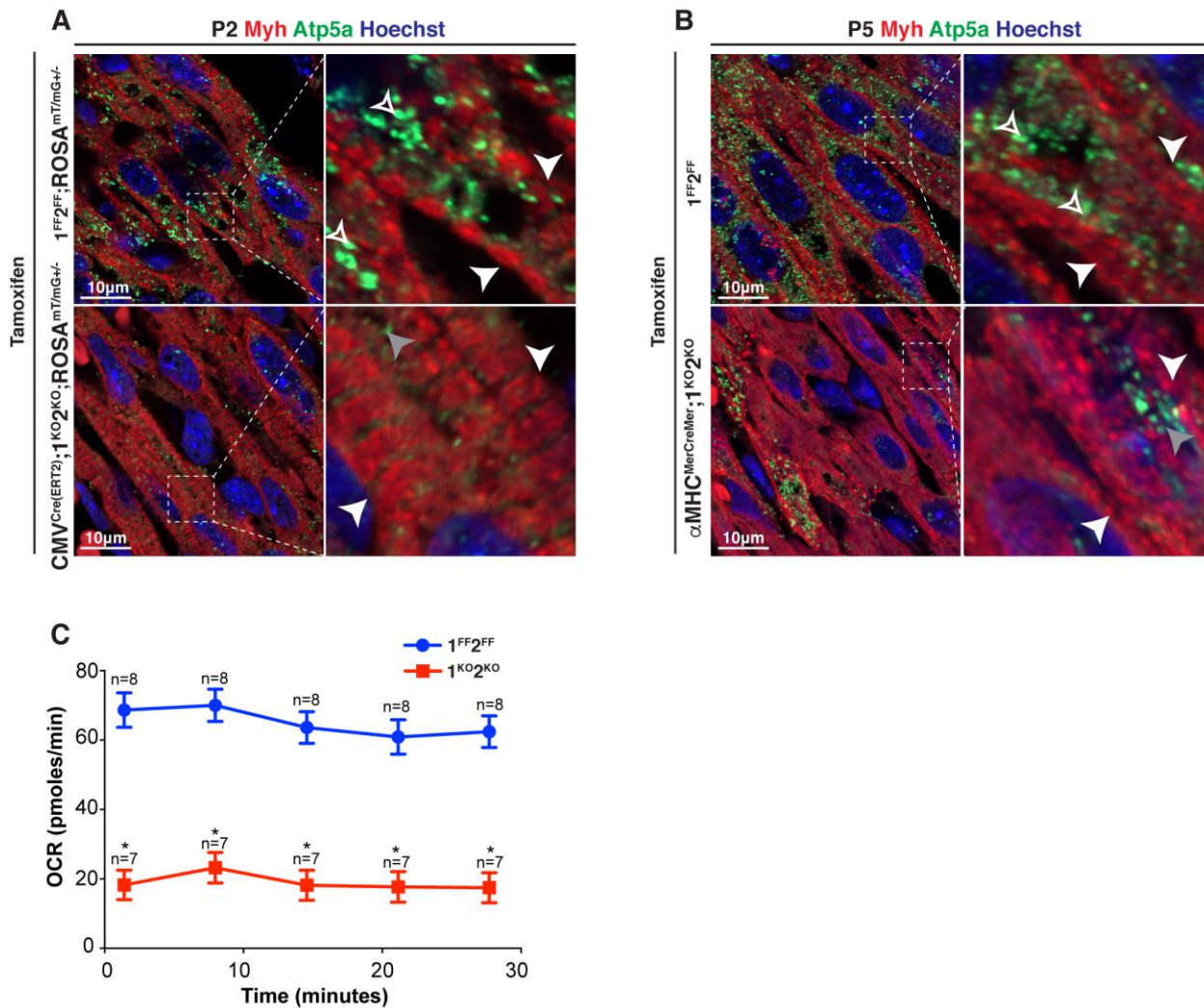


Fig. S3. Inducible loss of Hdac1 and Hdac2 in postnatal hearts lead to downregulation of critical mitochondrial protein and reduced oxygen consumption.

(A-B) Atp5a (Green) and Myh (Red) co-staining on tamoxifen treated $CMV^{Cre(ERT2)};I^{KO2^{KO}};ROSA^{mTmG+/-}$ (A), $\alpha MHC^{MerCreMer};I^{KO2^{KO}}$ (B), and $I^{FF2^{FF}}$ (A-B) P2 (A) and P5 (B) heart frontal sections with Hoechst nuclear counterstain. (solid white arrows, Myh⁺ contractile network; hollow white arrows, Atp5a⁺ cardiomyocytes; gray arrows, reduced Atp5a expression in cardiomyocytes). (C) Oxygen consumption rate (OCR) at multiple time points in neonatal P2 cardiomyocytes derived from P0 $I^{FF2^{FF}}$ hearts infected with control virus ($I^{FF2^{FF}}$) or with Cre-expressing virus ($I^{KO2^{KO}}$). Data represent the mean \pm SEM. *P<0.00003. Statistical significance determined using the Holm-Sidak method, with alpha = 0.05.

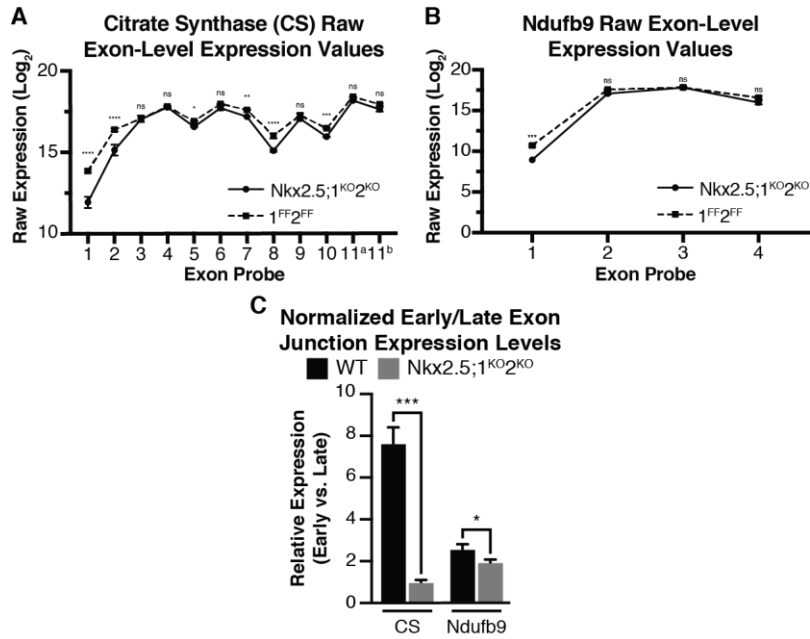


Fig. S4. Loss of Hdac1/Hdac2 causes downregulation of metabolic and cardiac gene programs without concordant upstream changes.

(A-B) Raw exon-level expression values (\log_2) for citrate synthase (*CS*, A) and *Ndufb9* (B) in *Nkx2.5;1^{KO2KO}* and *1^{FF2FF}* E10.5 PHTs. (C) RT-qPCR showing the relative abundance of *CS* or *Ndufb9* transcripts spanning an early exon junction (*CS* – Exon 1-2; *Ndufb9* – Exon 1-2) compared to late exon junction (*CS* – Exon 6-7; *Ndufb9* – Exon 3-4) in *Nkx2.5;1^{KO2KO}* and *1⁺⁺²⁺⁺* E10.5 PHTs.

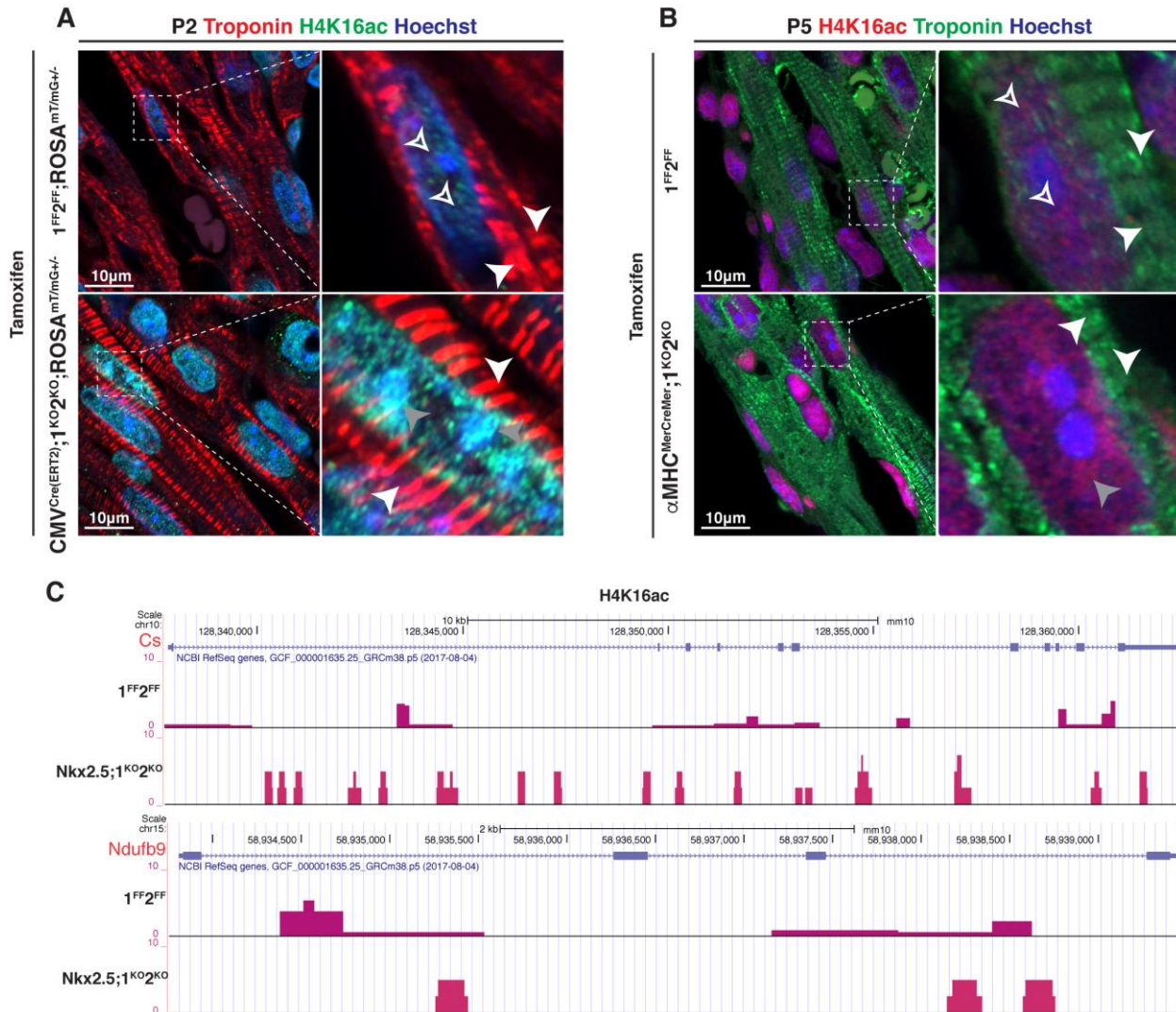


Fig. S5. Inducible loss of Hdac1 and Hdac2 in postnatal hearts leads to increased H4K16ac. (A-B) H4K16 and Troponin co-staining on tamoxifen treated $CMV^{Cre(ERT2)};I^{KO2}{}^{KO};ROSA^{mTmG+/-}$ (A), $\alpha MHC^{MerCreMer};I^{KO2}{}^{KO}$ (B), and $I^{FF2}{}^{FF}$ (A-B) P2 (A) and P5 (B) heart frontal sections with Hoechst nuclear counterstain. (solid white arrows, Troponin⁺ cardiomyocytes; hollow white arrows, H4K16ac⁺ cardiomyocytes; gray arrows, increased H4K16ac foci in cardiomyocytes). (C) Browser tracks of *Cs* (top) and *Ndufb9* (bottom) showing H4K16ac enrichment in $I^{FF2}{}^{FF}$ and $Nkx2.5;I^{KO2}{}^{KO}$ E10.5 primitive heart tubes.